P19

First Principles Study on the Switching Mechanism in Resistance Random Access Memory Devices

Hideaki Kasai, Susan Meñez Aspera, Hirofumi Kishi
Graduate School of Engineering, Osaka University
Precision Science & Technology and Applied Physics
Osaka, Japan
kasai@dyn.ap.eng.osaka-u.ac.jp

Nobuyoshi Awaya, Shigeo Ohnishi, Yukio Tamai
Sharp Corporation
Corporate Research and Development Group
Hiroshima, Japan

Abstract— **The role of Resistance Random Access Memory (RRAM) is recently becoming extremely important in the field of developing non-volatile memory devices. The foreseen relevance of RRAM in this field is attributed to the switching of the electronic properties from metal to insulator, and vice versa, of the transition metal oxides (TMOs) included in RRAM by a set and reset pulse voltage. However, conclusive clarifications on the switching mechanism have not yet been fully realized. In this study, by using first principles calculation based on density functional theory, we investigated RRAM's switching mechanism through analysis of the change in the electronic properties of the bulk TMOs resulting from oxygen vacancies and charge carrier trapping for two known TMOs materials used in RRAM, HfO_2 and CoO. We found that an oxygen vacancy row with charge carrier trapping creates a conduction path and therefore the transition from insulator to metal. In addition, we perform calculations for slab models of the TMOs in contact with Ta electrodes and hence investigate the effects of oxygen vacancies at the interface between the TMO layers and the electrode layer. From the obtained results, we confirmed that our investigations on activation energy barrier for oxygen vacancy migration are consistent with the experimental data of voltages required for switching.**

RRAM, TMO, First Principles Study

I. INTRODUCTION

Technological advancement in materials design is apparently geared towards the development of materials for devices that are miniature, perform intended function faster, productively cost efficient, and can be operated with low power. In the development of non-volatile memories, Resistance Random Access Memory (RRAM) [1-8] is seen to be very promising in the field of developing non-volatile memory devices. Transition metal oxides (TMOs) included in RRAM switch their properties between insulator and metal. This switching mechanism of RRAM has been recently becoming one of the extremely important subject in the field of developing RRAM, however, conclusive clarification on the switching mechanism has not yet been fully found. In this relation, we foresee the need to understand the switching mechanism through an indepth investigation of the electronic properties of TMOs whose important information can be used as a ground for designing materials.

Some studies related to RRAM suggest that the creation of a conduction path on TMOs, through defect formation, charge carrier trapping, metal atom migration, etc., might be responsible for the switching mechanism [9-13]. Our research group has also investigated the Mott transition [14-16] and the oxidative reaction [17-18] through experimental and theoretical approaches. In this study, we investigate the change on the properties of the TMOs (CoO and HfO_2) resulting from oxygen vacancies and charge carrier trapping around the oxygen vacancies for clarification of the switching mechanism. We find that an oxygen vacancy row and charge carrier trapping create a conduction path, and therefore, make the transition from insulator to metal. Moreover, we consider that it is of utmost necessity to investigate oxygen vacancy migration which has an important role in the switching mechanism of RRAM in relation to the oxygen vacancy row for the creation of the conduction path. With this, we investigate the activation energy barriers for oxygen vacancy migration in CoO and HfO_2. We confirm that our investigations on activation energy barrier for oxygen vacancy migration are consistent with the experimental data of voltages required for switching. Therefore, this study provides information on some electronic properties of TMOs responsible for the switching mechanism in RRAM.

II. METHOD

All calculations are performed within the DFT framework using the spin-polarized version of the Vienna ab initio simulation package (VASP) [19] with periodic boundary conditions in three directions. Nonlocal correction in the form of the generalized gradient approximation (GGA) [20] is included for the exchange-correlation functional. We use the projector augmented wave (PAW) [21-23] potential to describe the electron-ion interaction. For atomic and molecular oxygen, a 400eV cutoff energy yields an O_2 bond length of 1.23Å. The bulk CoO [24-26] and the bulk HfO_2 [27] are modeled by supercells shown in Figs. 1(a) and 1(b), respectively. These models contain the oxygen vacancy rows and are sampled by 1x1x15 k-point mesh generated by the Monkhorst-Pack scheme [28]. The slabs of CoO and HfO_2 in contact with Ta electrodes are modeled by supercells shown in Figs. 2(a) and 2(b), respectively. These models are sampled by 5x5x1 k-point mesh. The atomic geometries are optimized by quasi-Newton algorithm using Hellmann-Feynman forces. The optimization of the ionic positions is performed until the forces acting on each atom become less than 10^{-5}eV/Å. Effects of electron correlations beyond GGA are taken into account within the

978-1-61284-418-3/11/$26.00 © 2011 IEEE

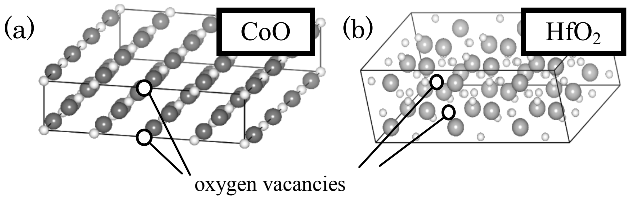

Figure 1. Supercells used in (a) the bulk CoO and (b) the bulk HfO$_2$ calculations with oxygen vacancies. The dark gray, light gray and white circles represent Co, Hf and O atoms, respectively.

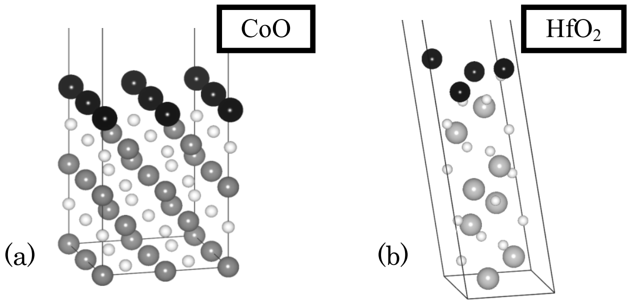

Figure 2. Slab models of the electrode/CoO and electrode/HfO$_2$. The dark gray, light gray and white circles represent Co, Hf and O atoms, respectively. The black circles represent the electrode atoms, Ta.

framework of GGA+U and the simplified (rotationally invariant) approach by Dudarev et al. [29] The Coulomb repulsion U=7eV and the local exchange interaction J=1eV are applied to correct the band gap of CoO. The Coulomb repulsion U=7.5eV and the local exchange interaction J=1eV are applied to correct the band gap of HfO$_2$. The GGA+U calculations of electronic density of states of CoO and HfO$_2$ lead to the energy gap of 2.5eV [30, 31] and 5.8eV [32], respectively.

III. RESULTS AND DISCUSSION

The switching mechanism of RRAM basically relies on the transition between the insulator to metal property of the TMO films sandwiched by the two metallic electrodes in capacitor-like RRAM devices. In this paper, we presume that this switching mechanism is attributed to the formation of an oxygen vacancy row and the occurrence of charge carrier trapping along the oxygen vacancy row of the TMO films. Investigations were done on two known metal oxide systems used in RRAM devices, CoO and HfO$_2$. We investigate the properties of bulk CoO and HfO$_2$ without oxygen vacancy, with the oxygen vacancy row and with the oxygen vacancy row and charge carrier trapping. The resulting band structures are shown in Figs. 3, 4 and 5. Fig. 3 confirms the insulator properties of the bulk CoO and HfO$_2$ without oxygen vacancy through the appearance of large bandgap around the Fermi level. On the other hand, the resulting band structures for the bulk CoO and HfO$_2$ with the oxygen vacancy rows, as shown in Fig. 4, show decrease of bandgap. Finally, we investigate the properties of bulk CoO and HfO$_2$ with the oxygen vacancy rows and by adding an extra electron per unit cell as a reference of the charge carrier trapping, as shown in Fig. 5. From this, we confirm the electrical conductivity of the bulk CoO and HfO$_2$ through the appearance of bands crossing with the Fermi level [33]. In addition, the electron density distributions along these bands, as shown in Fig. 6, represent that the presence of the oxygen vacancy rows and charge carrier trapping creates conduction paths around the vicinity of the oxygen vacancy rows that affect the electrical conductivity of the bulk CoO. Discontinuity within the aforementioned oxygen vacancy row changes the properties of the bulk CoO and HfO$_2$ back to insulator through the disappearance of bands that cross with the Fermi level.

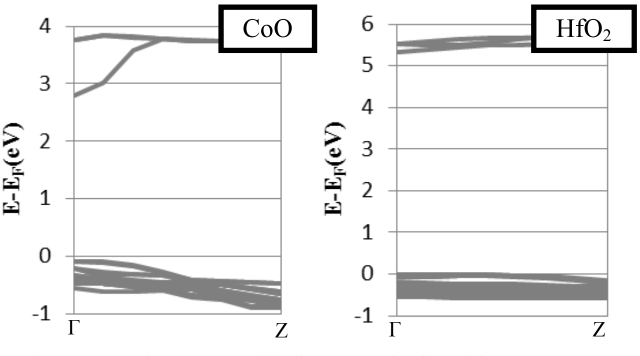

Figure 3. Band structures of bulk CoO and HfO$_2$ without oxygen vacancy.

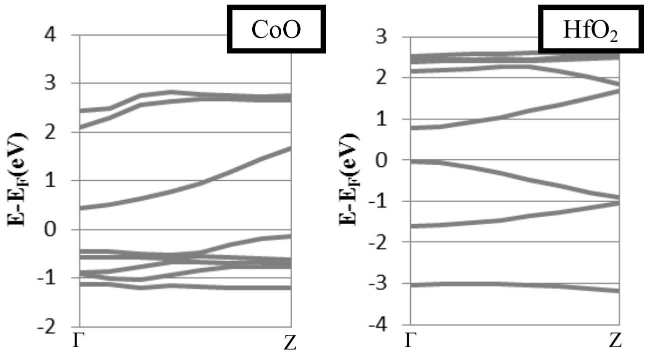

Figure 4. Band structures of bulk CoO and HfO$_2$ with the oxygen vacancy rows.

Through these, we consider that it is of utmost necessity to investigate oxygen vacancy migration which has an important role in the switching mechanism of RRAM in relation to the required oxygen vacancy row for the creation of the conduction path. Some studies related to RRAM suggest that the transition from insulator to metal is due to oxygen vacancy migration around the interface between electrode and

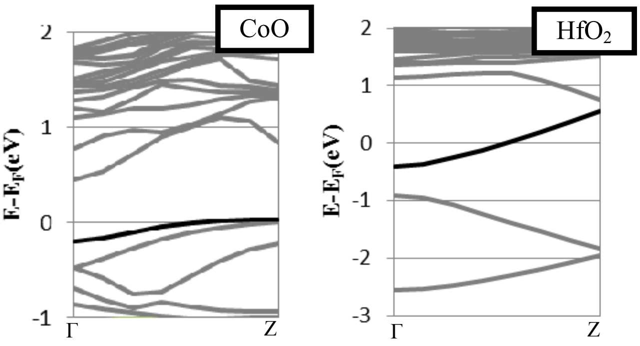

Figure 5. Band structures of bulk CoO and HfO$_2$ with the oxygen vacancy rows and charge carrier trapping. Bands crossing with the Fermi level are shown in darker shades.

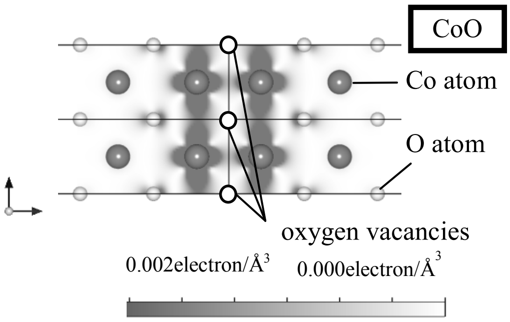

Figure 6. Electron density distribution along the band crossing with the Fermi level in the bulk CoO with the oxygen vacancy rows and charge carrier trapping.

TMO [34]. We therefore use the system of the CoO slab and the HfO_2 slab in contact with Ta electrodes [15] using the model represented in Fig. 2. The resulting density of states for each layer of the CoO slab and the HfO_2 slab are shown in Figs. 7 and 8, respectively.

From these figures we find that the interface layers of CoO (the first layer) and HfO_2 (the first and the second layers) have properties of metal and the lower layers have properties of insulator. From these, we assume that the creation of a conduction path through the formation of the oxygen vacancy row is via migration of oxygen vacancy from the interface to the lower layers. This switching mechanism is represented in Fig. 9. The insulating system (high resistance state) of RRAM is represented in Fig. 9 (a). In this case, an oxygen atom interrupts the conduction path between interface and lower layers which makes the system insulating. From this insulating system, an oxygen atom migrates to the interface layers through an application of a sufficient amount of set pulse voltage, which therefore makes the oxygen vacancy migrate to the lower layers thus converting the system to metallic [34]. The metallic system (low resistance state) of RRAM is represented in Fig. 9 (b). The oxygen vacancy connects the conduction path between interface and lower layers, and creates electrical conductivity within lower layers of CoO and HfO_2. A reset pulse voltage reverses the direction of the oxygen atom migration from the interface layers to the lower layers, thus migrating the oxygen vacancy from the lower layers to the interface layers which switches back the system to the insulating system.

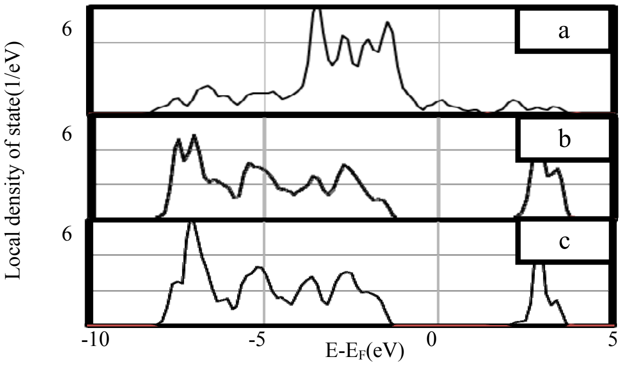

Figure 7. Density of states at different CoO layers in the Ta/CoO system. (a) the first, (b) second and (c) third CoO layers.

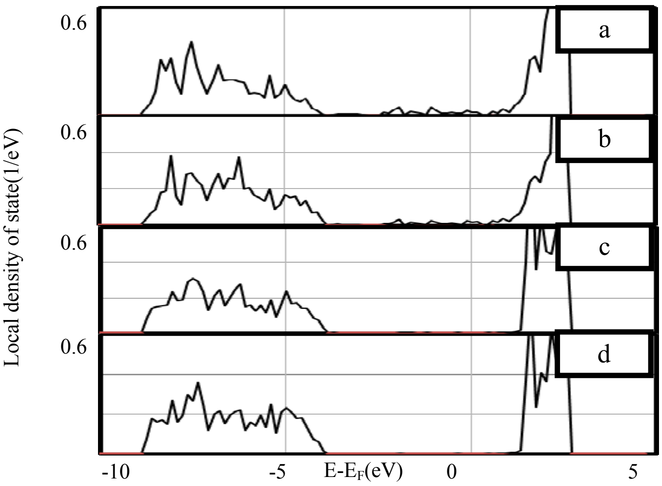

Figure 8. Density of states at different HfO_2 layers in the Ta/ HfO_2 system. (a) the first, (b) second, (c) third and (d) fourth HfO_2 layers.

These set and reset pulse voltages applied to the Ta/CoO/Pt and Ta/HfO_2/TiN system are investigated experimentally. Results shown in Table I represent that a low reset pulse voltage is needed to switch the system from a low resistance state to a high resistance state whereas a higher set pulse voltage is needed to convert the system from a high resistance state to a low resistance state. These results are compared with the activation energy barriers for oxygen vacancy migration around the interface between electrodes and TMOs (CoO and HfO_2), which are mentioned before as essential part of the switching mechanism in the TMOs. We use Climbing Image Nudged Elastic Band (CI-NEB) [35] method with 5 images of transition states to determine the most effective path for oxygen vacancy migration, and hence the activation energy barriers, for positions near the electrode-bulk TMO interface of the Ta/CoO and Ta/HfO_2 systems. The corresponding activation energy barriers are shown in Table II. Generally, we see that the barrier for conversion from a metallic system (low resistance state) to an insulating system (high resistance state) is less than the barrier for converting it vice versa. This is attributed to the fact that TMO is more stably occurring as an insulator than a material with metallic property. It is therefore easier to switch the system from a metal to an insulator than the other way around. These results are consistent with the results obtained from experimental analysis wherein reset pulse voltage is lower than set pulse voltage. This therefore supports the previously proposed mechanism of switching involving oxygen vacancy migration as the main component of the switching.

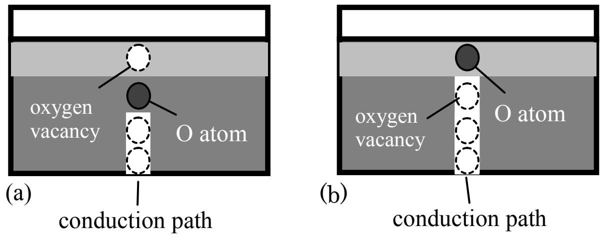

Figure 9. Illustration of the switching mechanism in the interface between a transition metal oxide and an electrode: (a) high, and (b) low resistance states of RRAM.

TABLE I. REQUIRED VOLTAGES FOR THE SWITCHING

Structure	**Ta / CoO / Pt**	**Ta / HfO_2 / TiN**
Size	5μm x 5μm	0.4μm x 0.4μm
Reset Pulse	1.7V	1.7V
	50ns	50ns
Resistance after Reset	300kΩ	200kΩ
Set Pulse	3V	3V
	50ns	50ns
Resistance after Set	10kΩ	9kΩ

TABLE II. ACTIVATION BARRIERS

Structure	**CoO**	**HfO_2**
From metal to insulator	2.5eV	0.2eV
From insulator to metal	2.9eV	1.3eV

IV. CONCLUSION

This paper has therefore clarified some properties of TMO resulting from oxygen vacancies and charge carrier trapping around the oxygen vacancies for clarification of the switching mechanism in RRAM devices. We find that an oxygen vacancy row and charge carrier trapping create a conduction path, which therefore makes the transition from insulator to metal. The switching mechanism is mainly attributed to the oxygen vacancy migration near the interface of the electrode-TMO layers triggered by the application of a set and reset pulse voltage.

ACKNOWLEDGMENT

This work is supported by the New Energy and Industrial Technology Development Organization's (NEDO) through the project entitled, 'Research and development of transition-metal oxides and its nanofabrication processes for ultra-high-density non-volatile memory'. Some of the calculations presented here are performed using the computer facilities of the Institute of Solid State Physics (ISSP) Super Computer Center (University of Tokyo) and the Cybermedia Center (Osaka University). The authors also acknowledge Dr. Wilson Agerico Diño, Dr. Hiroshi Nakanishi and Dr. Sumio Terakawa for fruitful discussions.

REFERENCES

[1] J. W. Park, J. W. Park, D. Y. Young, and J. K. Lee, J. Vac. Sci. Technol. A 23 (2005) 1309.

[2] S. Seo, M. J. Lee, D. H. Seo, S. K. Choi, D. S. Suh, Y. S. Joung, I. K. Yoo, I. S. Byun, I. R. Hwang, S. H. Kim, and B. H. Park, Appl. Phys. Lett. 86 (2005) 093509.

[3] S. Seo, M. J. Lee, D. H. Seo, E. J. Jeoung, D. S. Suh, Y. S. Joung, I. K. Yoo, I. R. Hwang, S. H. Kim, I. S. Byun, J. S. Kim, J. S. Choi, and B. H.Park, Appl. Phys. Lett. 85 (2005) 5655.

[4] A. Beck, J. G. Bednorz, Ch. Gerber , C. Rossel, D. Widmer, Appl. Phys. Lett. 77 (2000) 139.

[5] S. Q. Liu, N. J. Wu, A. Ignatiev, Appl. Phys. Lett. 76 (2000) 2749.

[6] R. Waser, M. Aono, Nature Mater. 6 (2007) 833.

[7] A. Sawa, Materials Today, 11 (2008) 28.

[8] K. Kinoshita, T. Tamura, M. Aoki, Y. Sugiyama, H. Tanaka, Jpn. J. Appl. Phys., 45 (2006) L991.

[9] M. Houssa, M. Tuominen, M. Naili, V. Afanas'ev, A. Stesmans, S. Haukka, M. M. Heyns, J.Appl. Phys., 87 (2000) 8615.

[10] M. J. Rozenberg, I. H. Inoue, M. J. Sa´nchez, Phy. Rev. Lett., 92 (2004) 178302.

[11] Y. C. Yang, F. Pan, F. Zeng, M. Liu, J. Appl. Phys. 106 (2009) 123705.

[12] J. Ozeki, H. Itoh, J. Inoue, J. Magn. Magn. Mater., 310 (2007) e644.

[13] N. Sasaki, K. Kita, A. Toriumi, Kentaro Kyuno, Jpn. J. Appl. Phys. 48 (2009) 060202.

[14] A. Okiji, H. Kasai, S. Terakawa, J. Phys. Soc. Jpn. 44 (1978) 1275.

[15] A. Okiji and H. Kasai, Surf. Sci. 86 (1979) 529.

[16] H. Kishi, T. Kishi, W. A. Diño, E. Minamitani, H. Akinaga, H. Nakanishi, H. Kasai, J. Comput. Theor. Nanosci. 5 (2008) 1976.

[17] Y. Tamai, H. Shima, H. Muramatsu, H. Akinaga, Y. Hosoi, S. Ohnishi, N. Awaya, Extended Abstracts of the 2008 International Conference on Solid State Devices and Materials, Tsukuba (2008) 1166-1167.

[18] M. David, R. Muhida, T. Roman, H. Nakanishi, W. Dino, H. Kasai, F. Takano, H. Shima, H. Akinaga, Vacuum 83 (2009) 599.

[19] G. Kresse, J. Furthmüller, Computer code VASP, Vienna, Austria,1999;
G. Kresse, J. Furthmüller, Comput. Mater. Sci. 6 (1996) 15;
G. Kresse, J. Hafner, Phys. Rev. B 47 (1993) 558;
G. Kresse, J. Furthmüller, Phys. Rev. B 54 (1996) 11169.

[20] J. P. Perdrew, J. A. Chevary, S. H. Vosko, K. A. Jackson, M. R. Pederson, D. J. Singh, C. Fiolhais, Phys. Rev. B 46 (1992) 6671.

[21] P.E. Blõchl, Phys. Rev. B 50 (1994) 17953.

[22] G. Kresse, D. Joubert, Phys. Rev. B 59 (199) 1758.

[23] P. E. Blochl, Phys. Rev. B 50 (1994) 17953.

[24] H. Shima, F. Takano, Y. Tamai, H. Akinaga, I. H. Inoue, Jpn. J. Appl. Phys., 46 (2007) L57.

[25] F. Takano, H. Shima, H. Muramatsu, Y. Kokaze, Y. Nishioka, K. Suu, H. Kishi, N. B. Alboleda Jr., M. David, T. Roman, H. Kasai, H. Akinaga, Jpn. J. Appl. Phys., 47 (2008) 6931.

[26] H. Shima, F. Takano, H. Muramatsu, H. Akinaga, Y. Tamai, I. H. Inque, H. Takagi, Appl. Phys. Lett. 93 (2008) 113504.

[27] X. Zhao, D. Vanderbilt, Phys. Rev. B 65 (2002) 233106.

[28] H. J. Monkhorst, J. D. Pack, Phys. Rev. B 13 (1976) 5188.

[29] S. L. Dudarev, G. A. Botton, S. Y. Savrasov, C. J. Humphreys, A.P. Sutton, Phys. Rev. B 57 (1998) 1505.

[30] U. D. Wdowika, D. Legut, J. Phys. Chem. Solids., 69 (2008) 1698.

[31] J. van Elp, J. L. Wieland, H. Eskes, P. Kuiper, G. A. Sawatzky, F. M. F. de Groot, T. S. Turner, Phys. Rev. B 44 (1991) 6090.

[32] V. V. Afanas'ev, A. Stesmans, F. Chen, X. Shi, S. A. Campbell, Appl. Phys. Lett., 81 (2002) 1053.

[33] H. Kasai, T. Kakuda, A. Okiji, Surf. Sci., 363 (1996) 428.

[34] A. Sawa, Mater. today, 11 (2008) 28.

[35] G. Henkelman, B.P. Uberuaga, H. Jonsson, J. Chem. Phys., 113 (2000) 9901.